Original Article

The downregulation of fibrinogen-like protein 1 inhibits the proliferation of lung adenocarcinoma via regulating *MYC*-target genes

Xi-Yang Tang[1#], Yan-Lu Xiong[1#], An-Ping Shi[2#], Ying Sun[1#], Qing Han[3], Yao Lv[3], Xian-Gui Shi[3], Milo Frattini[4], Jyoti Malhotra[5], Kai-Fu Zheng[1], Yu-Jian Liu[1], Tao Jiang[1], Nan Ma[6], Jin-Bo Zhao[1]

[1]Department of Thoracic Surgery, Tangdu Hospital, Air Force Medical University, Xi'an, China; [2]Department of Radiology and Functional and Molecular Imaging Key Lab of Shaanxi Province, Tangdu Hospital, Fourth Military Medical University (Air Force Medical University), Xi'an, China; [3]College of Basic Medicine, Air Force Medical University, Xi'an, China; [4]Laboratory of Molecular Pathology, Institute of Pathology (ICP), Cantonal Hospital (EOC), Locarno, Switzerland; [5]Rutgers Cancer Institute of New Jersey, New Brunswick, NJ, USA; [6]Department of Ophthalmology, Tangdu Hospital, Air Force Medical University, Xi'an, China

Contributions: (I) Conception and design: JB Zhao, YL Xiong; (II) Administrative support: JB Zhao, N Ma, T Jiang; (III) Provision of study materials or patients: Y Sun; (IV) Collection and assembly of data: XY Tang; (V) Data analysis and interpretation: JB Zhao, YL Xiong, XY Tang, KF Zheng, YJ Liu, XG Shi, Y Lv, M Frattini, J Malhotra; (VI) Manuscript writing: All authors; (VII) Final approval of manuscript: All authors.
[#]These authors contributed equally to this work.

Correspondence to: Jin-Bo Zhao. Department of Thoracic Surgery, Tangdu Hospital, Air Force Medical University, 569 Xinsi Road, Xi'an 710038, China. Email: zhaojinbo@aliyun.com; Nan Ma. Department of Ophthalmology, Tangdu Hospital, Air Force Medical University, 569 Xinsi Road, Xi'an 710038, China. Email: manan840808@163.com; Tao Jiang. Department of Thoracic Surgery, Tangdu Hospital, Air Force Medical University, 569 Xinsi Road, Xi'an 710038, China. Email: jiangtaochest@163.com.

Background: The mechanisms involved in the malignant progression of lung adenocarcinoma (LUAD) are still inconclusive. Fibrinogen-like protein 1 (*FGL1*) and *LAG3* are a pair of immune checkpoints that create an inhibitory immune microenvironment in tumors. However, other roles of *FGL1* in LUAD have not been extensively studied. Our study aims to explore the role of *FGL1* in the malignant progression of LUAD and to provide new therapeutic targets and strategies for LUAD treatment.

Methods: Differential gene expression of *FGL1* was analyzed using the Gene Expression Profiling Interactive Analysis (GEPIA), Oncomine, UALCAN, and Gene Expression Omnibus (GEO) databases. A pan-cancer analysis was conducted using the Oncomine, TIMER, and UALCAN databases. A total of 140 tumor tissues and paired normal tissues were collected, IHC and immunofluorescence staining were used to explore the expression of *FGL1*. GeneMANIA database and STRING database were used to analyze gene-gene interaction and protein-protein interaction, respectively. A mutation analysis was conducted using the cBioPortal database, and an immune infiltration analysis was conducted using the TIMER database. A survival analysis was carried out using the GEPIA and PrognoScan database. The knockdown of *FGL1* was confirmed by western blot (WB) and immunofluorescence staining. Cell proliferation was tested by cell cycle analysis and real-time cell analysis. RNA sequencing (RNA-seq) was used to explore the differential genes of *FGL1* knockdown in LUAD cells.

Results: Multiple databases showed that *FGL1* was highly expressed in LUAD. The results of IHC indicated that *FGL1* was highly expressed in the cytoplasm of LUAD cells. *FGL1* was negatively associated with immune infiltration in LUAD. The main mutation of *FGL1* is deep deletion, the altered group and high expression group indicated poor prognosis. The downregulation of *FGL1* lead to a significantly decreased percentage of PC9 cells in S phase, but had little effect on the proliferation of Jurkat T cells. RNA-seq and GSEA analysis indicated that the differential genes were mainly enriched in *MYC*-target genes, which suggested that the downregulation of *FGL1* inhibited cell proliferation by regulating *MYC*-target genes.

Conclusions: *FGL1* exerts in LUAD proliferation in addition to immune regulation. The downregulation of *FGL1* inhibits the proliferation of LUAD cells by regulating *MYC*-target genes. Thus, *FGL1* may be a

novel therapeutic target in LUAD.

Introduction

Lung cancer has the highest mortality rate of all cancers worldwide, with 75% of patients developing advanced disease and experiencing a survival of less than 18 months, median 5-year survival is about 22% (1,2). Immune checkpoints inhibitors inhibit the progression of tumors by regulating the immune microenvironment, and immune checkpoint inhibitors targeting programmed cell death 1 (*PD-1*) and programmed death-ligand 1 (*PD-L1*) have shown powerful effects in the treatment of various tumors, however, the effective rate of *PD-1* and *PD-L1* monotherapy and combination therapy for lung cancer is still only about 30% (3). It is of great significance to further study the role of other novel immune checkpoint genes in the development of lung cancer.

The mechanisms involved in the oncogenic progression of lung adenocarcinoma (LUAD) are still inconclusive; however, immune checkpoint genes may be involved in tumor progression (4). Bioinformatic analysis is conducted in multiple databases, and find that the expression difference of fibrinogen-like protein 1 (*FGL1*) is significant in LUAD, thus, we choose *FGL1* for research. *FGL1* is a member of the fibrinogen-associated protein (*FREP*) family, which is also called *FREP1*, *HRFREP-1* or *hepassocin* (5-8). *FGL1* is one of the ligands of lymphocyte-activation gene 3 (*LAG3*), which is highly expressed on the membrane of breast cancer cells and the cytoplasm in non-small cell lung cancer (NSCLC) cells (9,10). *FGL1* may regulate T cell-related immune functions when binding to *LAG3*; specifically, *FGL1* inhibits the proliferation of T cells and decreases the level of *TNF-α*, *IFN-γ* when *LAG3* is overexpressed (10). Therefore, *FGL1* and *LAG3* are considered to be a pair of immune checkpoints. In addition, *FGL1* may serve as an indicator of tumor prognosis: high expression of *FGL1* predicts poor overall survival (OS) in hepatocellular carcinoma (HCC) and gastric cancer (4,11).

However, the role of *FGL1* in LUAD is still unclear. In NSCLC, FGL1 may be associated with immune resistance and gefitinib resistance (12,13). In LKB1 overexpressed A549 lung cancer line, the knockdown of FGL1 may induce epithelial-mesenchymal transition (EMT) and be related with tumor metastasis, but the results may be influenced by LKB1 overexpression (14), thus, the role of FGL1 in LUAD warrants further exploration. Here, using bioinformatic analysis combined with experimental validation, we report the mechanism of *FGL1*'s involvement in the progression of LUAD, demonstrated the proliferative role of *FGL1*, which may provide the therapeutic target for immunotherapy of LUAD and help improve prognosis of patients. We present the following article in accordance with the MDAR reporting checklist (available at https://tlcr.amegroups.com/article/view/10.21037/tlcr-22-151/rc).

Methods

Gene Expression Profiling Interactive Analysis (GEPIA) analysis

The GEPIA database (http://gepia.cancer-pku.cn/) provides customizable tools for differential gene expression analysis, gene-related survival analysis, gene correlation analysis, tumor clinical staging, and pathological staging. The data in GEPIA include the results of RNA-seq data from The Cancer Genome Atlas (TCGA) and the Genotypic-Tissue Expression (GTEx) project (15). In this study, we used GEPIA to conduct a differential gene expression analysis including 17 immune checkpoint receptor genes and part of the corresponding ligand genes (16). We also used GEPIA to conduct an *FGL1*-related survival analysis and to explore the expression of *FGL1* in various LUAD clinical stages.

Oncomine analysis

The Oncomine database (www.oncomine.org) is a tumor microarray database that can analyze 18,000 cancer gene expression profiles, pathways, and networks from various published articles (17). We used the Oncomine database to conduct an *FGL1* pan-cancer analysis and an expression analysis of pathological subtypes.

UALCAN analysis

UALCN (http://ualcan.path.uab.edu) is an online tool for gene expression analysis, survival analysis, methylation, correlation, and pan-cancer analysis using data from TCGA, the Clinical Proteomic Tumor Analysis Consortium (CPTAC), and the Children's Brain Tumor Tissue Consortium (CBTTC) databases (18-20). We used UALCAN to conduct an *FGL1* pan-cancer analysis from TCGA samples.

cBioPortal analysis

The cBioPortal database is an online instrument for analyzing gene mutations, copy number alterations (CNAs), and mRNA and protein expression Z scores (21,22). We used the cBioPortal database to analyze *FGL1* mutations and conduct a mutation-related survival analysis.

GeneMANIA analysis

The GeneMANIA database (https://genemania.org/) can predict the function of target genes or gene sets and explore the interactive network of target genes (23). We used the GeneMANIA database to explore the gene-gene interaction network of *FGL1*.

Search Tool for the Retrieval of Interacting Genes (STRING) analysis

The STRING database (https://www.string-db.org/) is a database that allows exploration of target gene protein-protein interaction networks and performs functional enrichment analyses (24). We used the STRING database to explore the protein–protein interaction network of *FGL1*.

Tumor Immune Estimation Resource (TIMER) analysis

The TIMER database (http://timer.cistrome.org/) is an online tool that can be used to analyze the relationship between gene expression and tumor infiltration immune cells and the association between immune infiltrates and clinical outcome. TIMER can also be used to explore the association between gene expression and tumor features (25,26). We used TIMER to analyze the association between *FGL1* expression and immune infiltration and to conduct a *FGL1* pan-cancer analysis.

Gene Expression Omnibus (GEO) analysis

The GEO database (https://www.ncbi.nlm.nih.gov/geo/) is the largest database from which experiments, gene expression profiles, and array- and sequence-based data can be downloaded (27). We used GEO to conduct a *FGL1* differential expression analysis.

PrognoScan analysis

PrognoScan database (http://www.prognoscan.org/) provides a powerful platform for meta-analysis of the prognostic value of tumor markers, it performs the relationship between gene expression and prognosis like OS and disease free survival (DFS) (28).

Gene Set Enrichment Analysis (GSEA) analysis

The GSEA database (http://www.gsea-msigdb.org/gsea/index.jsp) is an online tool that can be used to determine the statistical significance of a predefined set of genes. It can also test the differential expression level of 2 samples and the enrichment of preset differential genes (29,30). We used the GSEA database to explore the enrichment of differential genes between *FGL1*-NC (negative control) and *FGL1*-KD (knockdown) and to identify the possible mechanisms of *FGL1*-mediated tumor progression.

Immunohistochemical staining

A total of 70 LUAD tissues and paired normal tissue were obtained from patients with LUAD who were treated surgically at Tangdu Hospital of the Air Force Medical University from 2013 to 2014, the inclusion criteria were following: (I) lung adenocarcinoma was diagnosed by pathological biopsy; (II) complete laboratory and imaging examinations were performed before surgery; (III) follow-up data are complete and available; (IV) there was no preoperative history of chemoradiotherapy. Exclusion criteria were following: (I) prior treatment including radiotherapy, chemotherapy or targeted therapy; (II) the presence of serious heart, lung and other important organ diseases, consciousness disorders or other systemic malignancies; (III) follow-up data were not available or laboratory and imaging tests were incomplete. The 140 samples were prepared as a 3 μm tissue microarray. Xylene I/II/III, absolute ethyl alcohol, and 75% and 85% alcohol were all used to dewax the tissue microarray. The

microarray was put into an autoclaved citric acid buffer (pH 6.0) to boil for 15 minutes; 3% hydrogen peroxide was used to block the activity of peroxidase for a 20-minute incubation, and an anti-*FGL1* polyclonal antibody (1:100 dilution; Proteintech, Wuhan, China) was used to incubate the microarray overnight at 4 ℃. After this, phosphate buffer saline (PBS) was used to wash the microarray 3 times. The microarray was then incubated at room temperature with a secondary antibody conjugated with horseradish peroxidase (HRP) (1:200 dilution; Servicebio, Wuhan, China) for 50 minutes. The microarray was washed 3 times, and 3,3-diaminobenzidine (DAB; Servicebio) was used for microarray staining. The microarray was then dehydrated and sealed after the nucleus was redyed by hematoxylin.

The study was conducted in accordance with the Declaration of Helsinki (as revised in 2013). The study was approved by the Ethics Committee of the Air Force Medical University (No. 202003-018). Written informed consent, which included agreement to the use personal clinical data and the collection of tissue and plasma samples, was signed by all patients before any study-related procedures began.

Immunofluorescence staining

A slide was prepared with cells at about 70% density. To prevent the antibody from flowing away, a histochemical pen was used to draw a circle in the center of the slide where the cells were evenly distributed. Then 100 µL of membrane breaking solution (Servicebio) was added, and the slide was incubated at room temperature for 20 minutes. PBS was used to wash the slide 3 times, and the slide was incubated overnight at 4 ℃ with an anti-*FGL1* polyclonal antibody (1:100 dilution; Proteintech). After that, the slide was incubated at room temperature with a secondary antibody for 50 minutes and then sealed by Antifade Mounting Medium after the nucleus was redyed by 4',6-diamidino-2-phenylindole (DAPI).

Cell culture and FGL1 knockdown

PC9 lung cancer cells and HCC827 lung cancer cells (human; iCell Bioscience Inc., Shanghai China) were cultured in RPMI 1640 (Gibco, Shanghai, China) with 10% fetal calf serum at 37 ℃ in 5% CO_2. Jurkat T cells (human; iCell Bioscience Inc. Shanghai China) were cultured in RPMI 1640 with 12% fetal calf serum at 37 ℃ in 5% CO_2. The *FGL1* small interfering RNA (siRNA) sequences were as follow: (I) 5'-GGAGGAGGATGGACTGTAA-3'

and (II) 5'-GTGGGCTAGTCACCAAAGA-3'. These oligonucleotides were synthesized by RiboBio (Guangzhou, China). The expression of *FGL1* was knocked down stably in PC9 and HCC827 lung cancer cells by pHBLV-U6-FGL1-shRNA-EF1a-EGFP-T2A-PURO (Hanbio Tech, Shanghai, China). The sequences of the *FGL1* stable knockdown were: (I) 5'-GGAGGAGGATGGACTGTAA-3' and 5'-TTACAGTCCATCCTCCTCC-3' and (II) 5'-GTGGGCTAGTCACCAAAGA-3' and 5'-TCTTTGGTGACTAGCCCAC-3'.

Cell co-culture

Direct co-culture was performed in 6-well plates. PC9 cells ($5×10^5$) were seeded and cultured in each well of the 6-well plate in RPMI 1640 supplemented with 10% FBS for 24 hours, and then the PC9 cells were transfected with empty or *FGL1*-knockdown vectors. Jurkart T cells ($5×10^5$) were added directly to tumor cells. Three mL RPMI 1640 supplemented with 12% FBS was placed in each well and co-cultured for the next 36 hours, and then the PC9 cells and Jurkat T cells were collected for each cell cycle experiment (31).

Western blot (WB) analysis

The total protein was collected using a total protein collection kit (Invent Biotechnologies Inc., Plymouth, MN, USA). Cells were cleaved by a SD-001 buffer in the kit on ice for 15 minutes, and the lysate was centrifuged at 12,000 r/min for 30 seconds. An appropriate 5× protein loading buffer was added and boiled for 10 minutes. A bovine serum albumin (BSA; Beyotime, Shanghai, China) kit was used to estimate the contents of the extracted protein. According to the concentration of the collected protein, the appropriate protein was added to electrophorese through 10% SDS-polyacrylamide gel. The protein was transferred from the gel to the NC membrane by electrophoresis at 300 mA for 60 minutes and blocked at room temperature by QuickBlock (Beyotime, Shanghai, China). An anti-*FGL1* polyclonal antibody (1:250 dilution; Proteintech) was used for overnight incubation at 4 ℃. After that, the membrane was incubated at room temperature with a secondary antibody for 60 minutes and then incubated in a chemiluminescent HRP substrate (Millipore, USA) for 1 minute after being washed 3 times with a tris-buffered saline with Tween 20 (TBST). Finally, the membrane was exposed to film in a visualizer (Tanon, China).

408

Tang et al. FGL1 promotes LUAD proliferation via *MYC*-target genes

Cell proliferation analysis

All cells were collected and resuspended by 1 mL RPMI 1640 (Gibco), and the density of cells was measured by an electronic cell counter (Olympus, Tokyo, Japan). Six thousand cells with 150 μL RPMI 1640 were added to each hole in an E-Plate (Agilent, Shanghai, China). Then the plate was put into a real-time cell analyzer (Agilent, Shanghai, China), and the analysis of cell proliferation was completed within 120 hours.

Cell cycle analysis

All cells were collected and resuspended in ice-precooled 70% alcohol. RNaseA (Solarbio, Beijing, China) was added to eliminate the effects of RNA, cells were stained by propidium iodide (PI) for 10 minutes, cell cycle was analyzed by flow cytometry at 488 nm, and the results were analyzed by ModFit software.

Colony formation

PC9 and HCC827 cells were collected and seeded in 6-well plates (600/well). After 2 weeks, the plate was washed 3 times with PBS, the cells were fixed by methanol for 20 minutes and stained by crystal violet for 30 minutes, and the plate was dried using a blower.

mRNA-seq and analysis

Three samples of *FGL1*-NC and FGL1-KD cells were collected by TRIzol Reagent (Thermo Fisher Scientific, Waltham, MA, USA) and submitted to LC-Bio (Zhejiang, China) for mRNA-seq and analysis. A volcano map and bubble diagram were created using LC-Bio (https://www.lc-bio.cn/) and R language version 4.1 (The R Foundation for Statistical Computing, Vienna, Austria).

Statistical analysis

SPSS 26.0 software (IBM Corp., NY, Armonk, USA) was used to analyze the results of *FGL1* expression between various group. A Student's *t*-test was used to assess the relationship between *FGL1* expression in the GSE dataset and cell cycle analysis. A least significant difference (LSD) *t*-test was used to assess the statistical significance of the cell index between various groups in the cell proliferation trial. A P value of <0.05 was considered statistically significant.

Results

## FGL1 was highly expressed in LUAD

To date, 17 immune checkpoints and corresponding ligands have been reported to mediate tumor metastasis (16). To investigate the immune checkpoint genes that play a role in the development of LUAD, we explored the mRNA expression of 19 ligands (*Figure 1A*) and the corresponding 17 receptors (*Figure 1B*) in LUAD, lung squamous carcinoma (LUSC), and normal samples from the GEPIA database (Figures S1,S2). *FGL1* (one of the ligands of LAG3) was found to be significantly highly expressed in LUAD but not in LUSC when compared to normal samples.

Next, we explored the expression of *FGL1* in various lung cancer subtypes and further confirmed the high expression of *FGL1* in LUAD (*Figure 1C*). To understand the expression of *FGL1* in various tumors, the pan-cancer analysis of *FGL1* was carried out using the Oncomine, TIMER, and UALCAN databases. The results showed that the expression of *FGL1* was significantly overexpressed in LUAD, prostate adenocarcinoma (PRAD), and ovarian serous surface papillary carcinoma, but not in LUSC, and the results were consistent across all 3 databases (*Figure 1D*). Further, we compiled 3 GSE datasets (GSE 10072, GSE 33532, and GSE 32863) to explore the expression of *FGL1* in LUAD. Compared to that in normal samples, higher *FGL1* expression was found in LUAD (P<0.001 in GSE 10072; P<0.0001 in GSE 33532 and 32863); moreover, the Oncomine meta-analysis showed higher *FGL1* expression in LUAD compared to that in normal tissues (P=0.005; *Figure 1E*). A total of 70 LUAD tissues, 70 LUSC tissues, and paired 140 normal tissues were stained as a tissue microarray. The results confirmed that the *FGL1* expression level was indeed higher in LUAD compared to that in LUSC and in paired normal tissues (P<0.001). However, we also found high expression of *FGL1* in LUSC samples (*Figure 1F*). In addition, the staining showed that *FGL1* was mainly accumulated in the cytoplasm of LUAD cells.

Interaction analysis, genetic alteration, and immune infiltration analysis of FGL1 in LUAD

The gene-gene interactive network of *FGL1* was constructed by the GeneMANIA database (*Figure 2A*). *FGL1* was surrounded by 20 genes that were associated with *FGL1* in the GeneMANIA network categories of physical interaction, co-expression, predicted, co-localization,
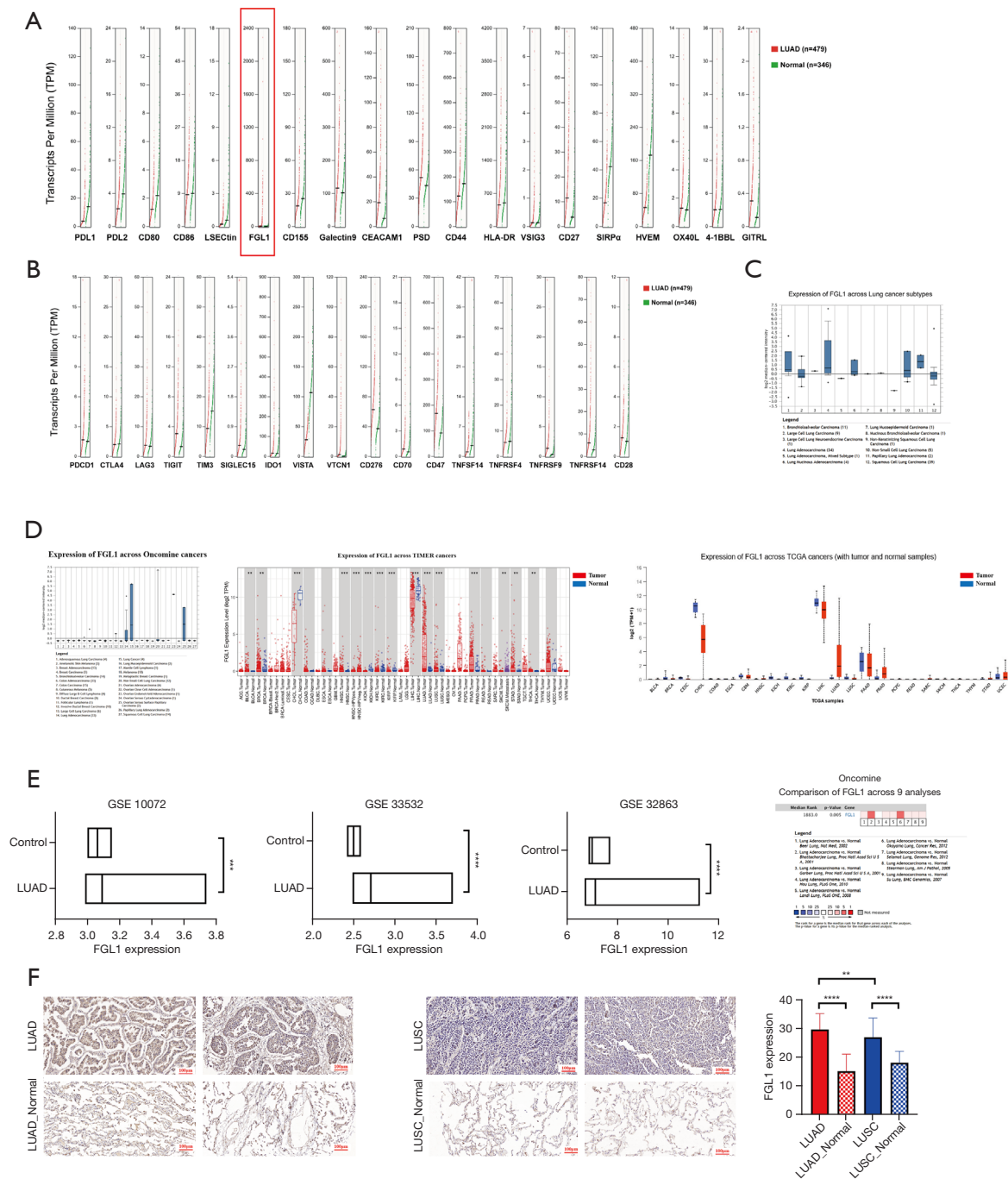
Figure 1 The differential expression and pan-cancer analysis of *FGL1* in multiple databases, confirmed by tissue microarray immunohistochemical staining. (A,B) The mRNA expression of 19 ligands (A) and the corresponding 17 receptors (B) were explored in LUAD; the differential expression of *FGL1* is significant and selected as the target gene. (C) The expression of *FGL1* in various lung cancer subtypes, the number in the brackets referred to the number of articles corresponding to the tumor. (D) The pan-cancer analysis of *FGL1* were made by the Oncomine, TIMER, and UALCAN databases, the number in the brackets referred to the number of articles corresponding to the tumor. (E) 3 GSE data sets (GSE 10072, GSE 33532, and GSE 32863) and Oncomine meta-analysis were used to explore the expression of *FGL1* in LUAD. (F) 70 LUAD, 70 LUSC tissues, and 140 paired normal tissues were stained as a tissue microarray by immunohistochemical staining, and we confirmed the expression level of *FGL1*. **, P<0.01; ***, P<0.001; ****, P<0.0001. *FGL1*, fibrinogen-like protein 1; LUAD, lung adenocarcinoma.
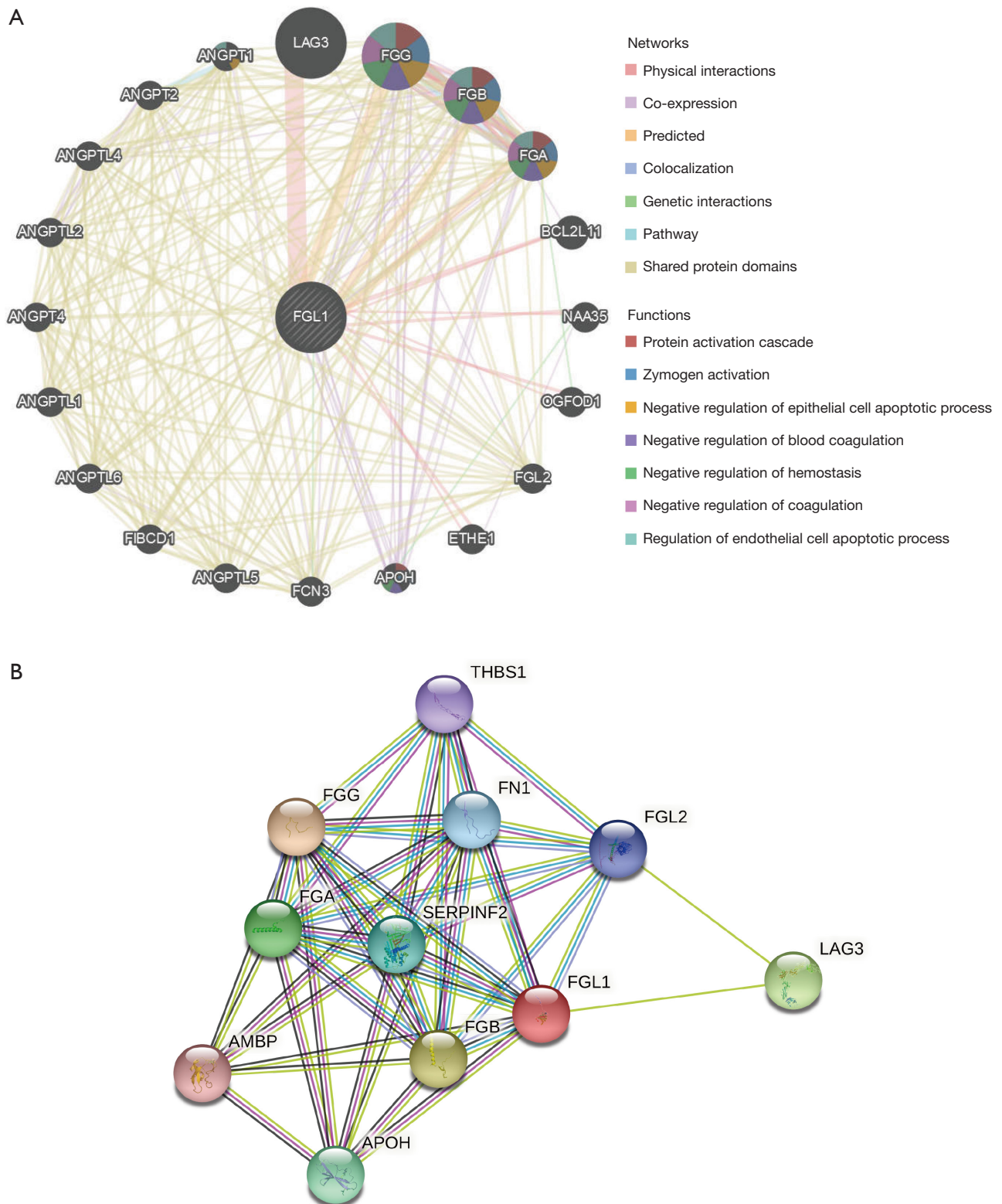
Figure 2 The interactive network of *FGL1*. (A) The gene-gene interactive network of *FGL1* was constructed by the GeneMANIA database. (B) The protein-protein interactive network was constructed by the STRING database. *FGL1*, fibrinogen-like protein 1.
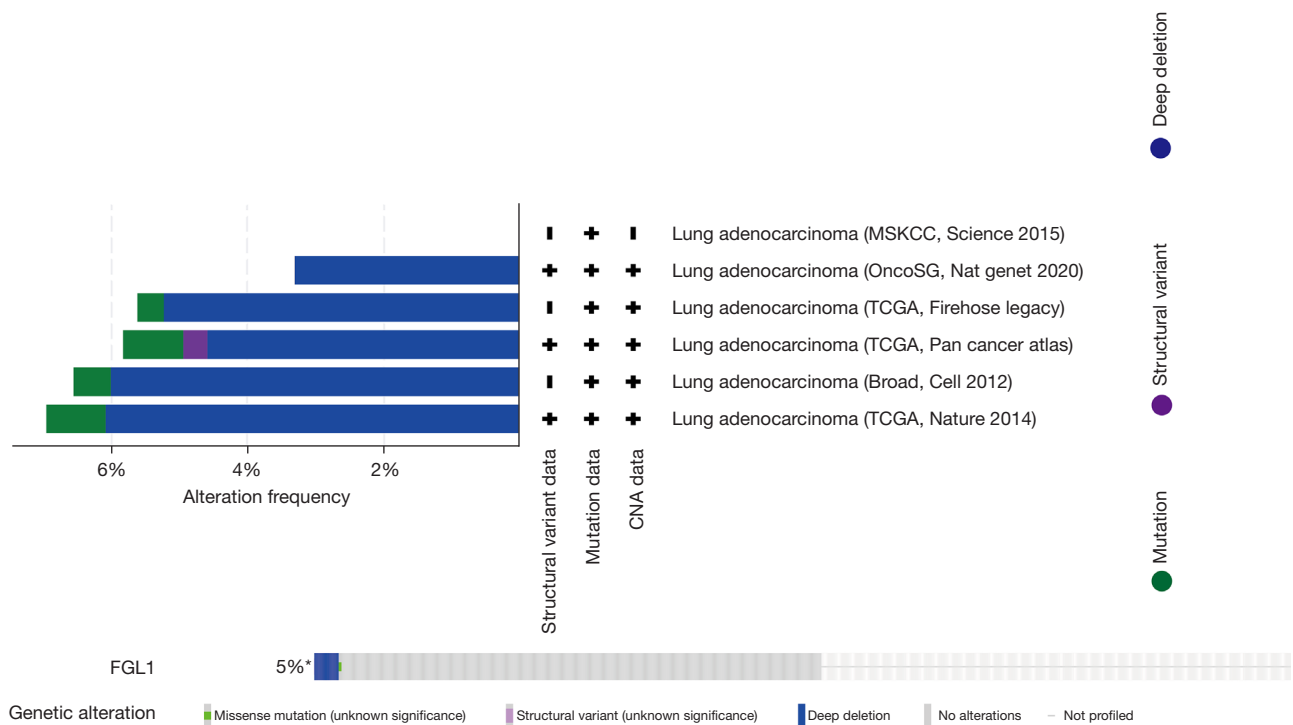
Figure 3 The genetic alteration of *FGL1* was presented by the cBioPortal database. +, the article included provides the corresponding data; –, the article included not provides the corresponding data; 5%*, the alteration frequency of deep deletion is 5%, significant in all alterations. *FGL1*, fibrinogen-like protein 1.

genetic interaction, pathway, and shared protein domains. The top 5 genes associated with *FGL1* were *LAG3*, fibrinogen gamma chain (*FGG*), fibrinogen beta chain (*FGB*), fibrinogen alpha chain (*FGA*), and angiopoietin 1 (*ANGPT1*). Among these genes, *LAG3* was tightly related to *FGL1* in physical interaction; however, the functions of *FGL1* and *LAG3* were still unclear. The interaction between *FGL1* and the other 4 genes might involve protein activation cascade, zymogen activation, negative regulation of the epithelial cell apoptotic process, blood coagulation, hemostasis, coagulation, and the regulation of the endothelial cell apoptotic process.

The protein-protein interactive network was constructed by the STRING database. As shown in *Figure 2B*, there were 10 proteins associated with *FGL1*.

The genetic alteration of *FGL1* was analyzed by the cBioPortal database. We analyzed 1,905 samples of patients with LUAD from 6 datasets in the cBioPortal database, and the results indicated that the main mutation type of *FGL1* was deep deletion (*Figure 3*).
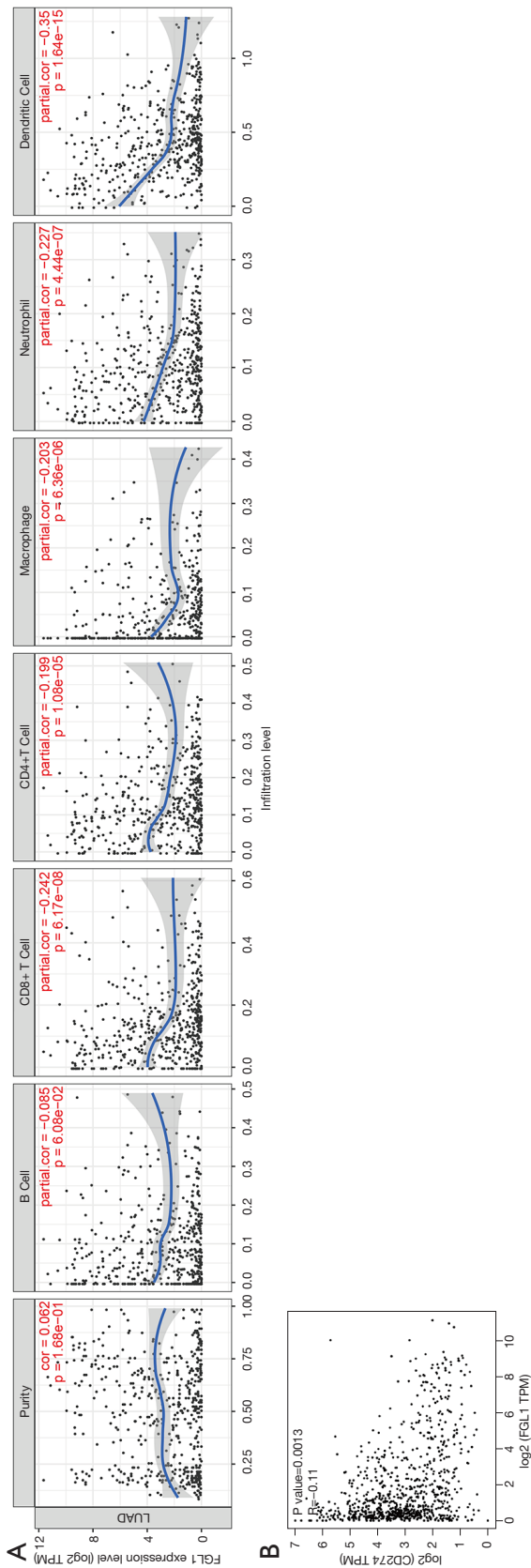
Immune infiltration related to *FGL1* was analyzed by the TIMER database. The *FGL1* expression level in LUAD was

negatively associated with immune infiltration, including the infiltration level of cytotoxic T cells (CD8+ T), T helper cells (CD4+ T), macrophages, neutrophil cells, and dendritic cells (*Figure 4A*). Further, the correlation analysis between *FGL1* and *PD-L1* in mRNA level has predicted by GEPIA common database, the P value of *FGL1/PD-L1* correlation analysis is significant but not for R value (*Figure 4B*). Thus, *FGL1* may synergize with *PD-L1* in tumor immune inhibition.

The high expression and deep deletion mutation of FGL1 were associated with the poor prognosis of patients with LUAD

The survival analysis of *FGL1* in LUAD was performed by the GEPIA database, with group cutoff defined as quartile. *FGL1* expression was a risk factor for OS and disease-free survival (DFS) of patients with LUAD (HR =1.5). The high expression of *FGL1* indicated poor prognosis of patients with LUAD (DFS, P=0.05; OS, P=0.056; *Figure 5A,5B*). Similar results were proved in dataset GSE 31210, analyzed by PrognoScan database, *FGL1* was negative associated with LUAD patients OS [P=0.009, HR (95% CI): 1.34 (1.04–1.73),

Figure 4 *FGL1*-related immune infiltration and the correlation analysis with *PD-L1*. (A) Immune infiltration related to *FGL1* was analyzed by the TIMER database. (B) The correlation analysis of *FGL1* and *PD-L1* (*CD274*) (GEPIA). *FGL1*, fibrinogen-like protein 1; PD-L1, programmed death-ligand 1; GEPIA, Gene Expression Profiling Interactive Analysis.
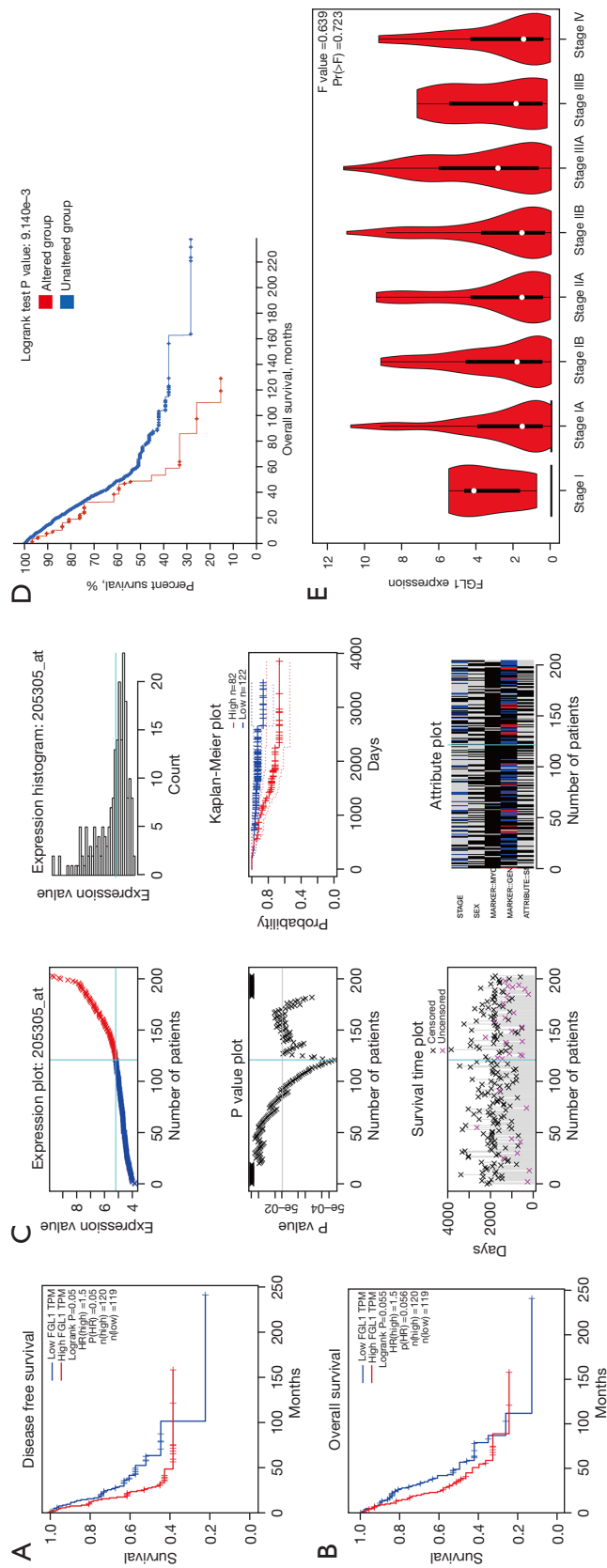
Figure 5 The survival analysis of *FGL1* in LUAD. (A,B) The survival analysis between *FGL1* expression and DFS (A), OS (B) in the GEPIA database. (C) The expression plot and survival analysis of GSE 31210, analyzed by PrognoScan database. (D) The survival analysis between *FGL1* deep deletion mutation and OS. (E) The expression of *FGL1* in various clinical stages. *FGL1*, fibrinogen-like protein 1; LUAD, lung adenocarcinoma; DFS, disease-free survival; OS, overall survival.

Figure 5C, https://cdn.amegroups.cn/static/public/tlcr-22-151-1.xls]. The cBioPortal OS analysis indicated that the prognosis of the altered group (deep deletion) was significantly poorer than that of the unaltered group (P=9.141e-3; *Figure 5D*). In addition, we used the GEPIA database to analyze *FGL1* expression in various LUAD clinical stages. The results showed that *FGL1* expression in different clinical stages was not statistically significant (*Figure 5E*).

The knockdown of FGL1 affected MYC-target genes

siRNA and short hairpin RNA (shRNA) were used to construct *FGL1* knockdown with transient transfection and stable transfection in a cell line of PC9 and HCC827 lung cancer cells. WB was used to confirm the knockdown of *FGL1* in PC9 and HCC827 lung cancer cells. The results showed that *FGL1* was knocked down in the KD-1 and KD-2 groups but not in the NC group. Immunohistochemical staining was used to confirm the knockdown of *FGL1* in PC9 lung cancer cells (*Figure 6A,6B*).

As previously mentioned, the cells were co-cultured for 36 hours. According to the RNA-seq data of the PC9 cells and Jurkat T cells, we found that the knockdown of *FGL1* upregulated 953 genes and downregulated 408 genes in PC9 cells (*Figure 6C*) but that the influence on Jurkat T cells was not significant (*Figure 6D*). GSEA analysis showed that these differential genes in PC9 cells were mainly enriched in *MYC_targets_v1/v2* genes with the highest significance compared to other signal pathways (*Figure 6E*), which is a set of genes associated with cell cycle, apoptosis, and tumor progression (32). These differential genes were also enriched in some signal pathways like oxidative phosphorylation, mTORC1 signaling, and unfolded protein response. Based on these results, we concluded that the downregulation of *FGL1* mainly inhibited the cell proliferation of PC9 cells via regulating *MYC*-target genes.

Then, RNA-seq was used to confirm the differential expression of *MYC*-target genes in HCC827 cells after *FGL1* knockdown, the enrichment plots showed that the knockdown of *FGL1* was tightly associated with of *MYC_targets_v1/v2* genes (Figures S3,S4), the results of heat map also showed that compared to NC group, the differential expression of most *MYC_targets_v1/v2* genes in *FGL1* knockdown group was significant (Figures S5,S6).

The knockdown of FGL1 inhibited cell proliferation

After the transfection of empty or *FGL1*-knockdown

vectors, PC9 cells were added in a 6-well plate to co-culture with Jurkat T cells for 36 hours and then collected for cell cycle experiment. The results showed that for PC9 cells, the percentage of cells in S phase in the Co-Culture_LUAD-KD group was significantly decreased compared to that in the Co-Culture_LUAD-NC group (P<0.0001); however, for Jurkat T cells, the G0/G1, S, and G2/M phases were not statistically significant (*Figure 7A*). To eliminate the effects of co-culture, we seeded the PC9 cells of LUAD-NC and LUAD-KD in another 6-well plate, and the cell cycle analysis similarly showed that the percentage of cells in S phase in the LUAD-KD group was significantly decreased (*Figure 7B*).

Cell proliferation assessment was performed by a real-time cell analyzer, which presented the real-time conditions of cell proliferation. We analyzed the cell proliferation of PC9 cells within 120 hours (*Figure 7C*), choosing to analyze the cell index between various groups at 80 hours and 100 hours, and HCC827 cells within 80 hours, choosing to analyze the cell index between various groups at 60 hours and 80 hours. Compared to those in the *FGL1*_NC groups, we found that the cell indexes in *FGL1*_KD1 and *FGL1*_KD2 were statistically significantly smaller in both PC9 and HCC827 cells (*Figure 7C*). Colony formation assay was also performed to evaluate the cell proliferation of PC9 and HCC827 cells. After a 2-week culture of 600 cells in each well, the cell count of the KD1 and KD2 groups were significantly smaller than that of the NC group (*Figure 7D*), which indicated that the low expression of *FGL1* could significantly inhibit the proliferation of LUAD cells.

Discussion

With the development of target therapy and immunotherapy, the outcomes of LUAD have been improved significantly. However, the mechanisms of malignant progression in LUAD are still unclear. In our study, we found that *FGL1*, one of the immune checkpoint genes, could promote the tumor progression in LUAD; specifically, we confirmed that *FGL1* is highly expressed in the cytoplasm of LUAD cells and promotes the proliferation of LUAD cells via regulating *MYC*-target genes.

FGL1 is associated with immune inhibition and tumor progression. *FGL1* may mediate tumor immune inhibition by affecting the function of T cells and the production of cytokines on condition that *LAG3* is overexpressed (10,33). Similar effect can be found when *PD-L1* interact with PD-1 (34). The correlation analysis between *FGL1* and
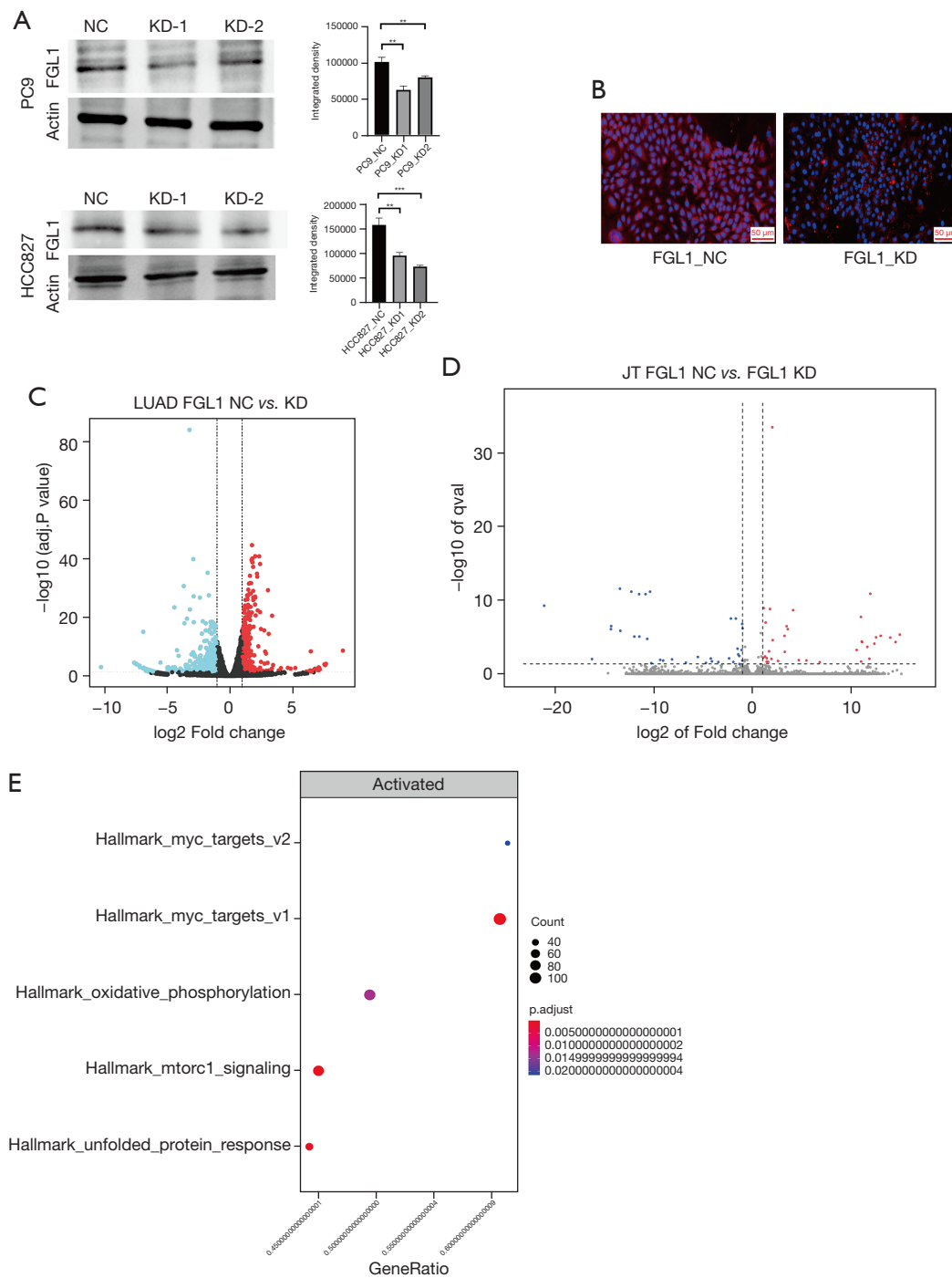
Figure 6 The knockdown of *FGL1* and RNA-seq results. (A) The knockdown of *FGL1* confirmed by western blot. (B) The knockdown of *FGL1* confirmed by immunofluorescent staining. (C) Volcano map of differential gene changes in PC9 cells after *FGL1* knockdown. (D) Volcano map of differential gene changes in Jurkat T cells after *FGL1* knockdown. (E) The enrichment of differential genes in PC9 cells, analyzed by GSEA. **, P<0.01; ***, P<0.001. NC, negative control; KD, knockdown; LUAD, lung adenocarcinoma; *FGL1*, fibrinogen-like protein 1.
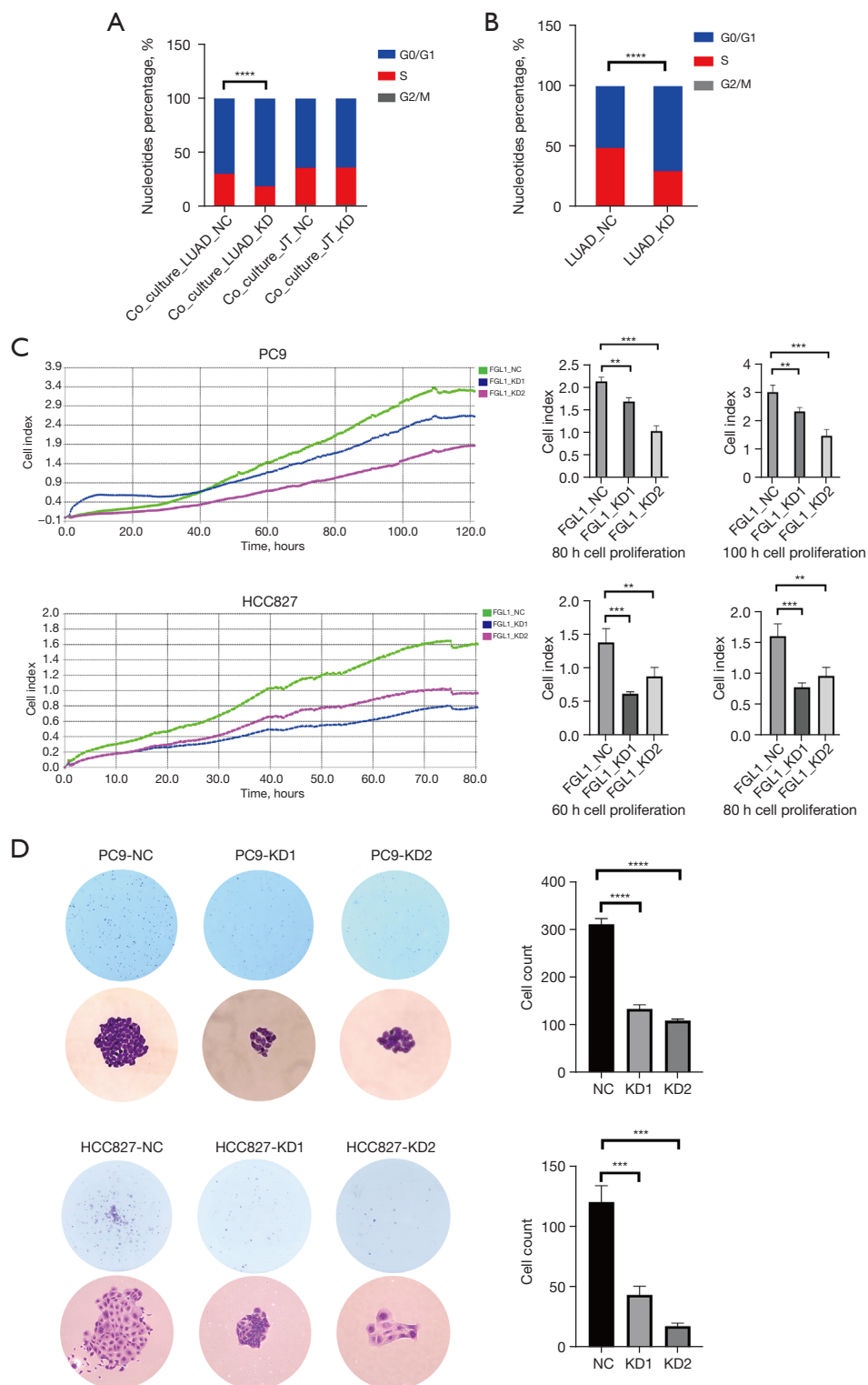
Figure 7 The experiments related to cell proliferation. (A,B) Effects of *FGL1* knockdown on the cycle of PC9 cells and Jurkat T cells. (C) Real-time cell analyzer presents the real-time condition of cell proliferation. (D) Colony formation confirms the cell proliferation of PC9 cells and HCC827 cells, the magnifications in the figure are 40× and 200×, respectively, both of them were stained with crystal violet. **, P<0.01; ***, P<0.001; ****, P<0.0001. NC, negative control; KD, knockdown; LUAD, lung adenocarcinoma; *FGL1*, fibrinogen-like protein 1.

PD-L1 in mRNA level also prove that *FGL1* may synergize with *PD-L1* in tumor immune inhibition. Recently, more evidences support that *FGL1* may play significant role in tumor proliferation, migration and invasion, including colon cancer, gastric cancer and HCC, also, the high expression of *FGL1* is positively associated with poor prognosis of tumor patients (4,10,35). Especially, in lung cancer, *FGL1* may be involved in tumor progression and drug resistance: first, in *LKB1* overexpression lung cancer, *FGL1* exerts in inhibiting tumor proliferation; second, *FGL1* is highly expressed in lung cancer with *EGFR* mutation, which confers gefitinib resistance by regulating the *PARP1/caspase 3* pathway (12), third, in the lung cancer subtype of *EGFR*, *ERBB2*, *KRAS* and the receptor tyrosine kinase *RET* mutation, *FGL1* can also be found overexpressed, the high expression of *FGL1* in the subtype can be attributed to the mutation of *STK11* and the inactivation of *AMPK*, which further promote the upregulation of *HNF1A*, and the high expression of *FGL1* can predict the therapeutic effect of docetaxel and mTOR inhibitors (36), however, the specific mechanism of *FGL1*-mediated proliferation for LUAD is still unknown, which is our study aim. Our study demonstrates that *FGL1* promotes the proliferation of LUAD by regulating *MYC* signal pathway. First, *FGL1* is highly expressed in the cytoplasm of LUAD cells. We analyzed the expression of all immune checkpoint receptors and ligand genes in LUAD and LUSC and found that *FGL1* is highly expressed in LUAD compared to LUSC and normal tissues. The analysis was conducted using multiple databases, including GEPIA, UALCAN, Oncomine, GEO, and TCGA, and the results consistently indicated the high expression of *FGL1* in LUAD. Immunohistochemical staining of a tissue microarray confirmed that high protein level of *FGL1* in the cytoplasm of LUAD cells. Although we also found high protein level of *FGL1* in LUSC samples, the results of GEPIA, UALCAN and TCGA databases all showed the low mRNA level of *FGL1* in LUSC. The difference between mRNA level and protein level could be attributed to post-transcriptional regulation. These results suggest that *FGL1* may exert its biological function in the cytoplasm of LUAD cells.

Second, *FGL1* was negatively associated with immune infiltration and predicted the poor prognosis of patients with LUAD. The immune infiltration analysis of *FGL1* indicated that *FGL1* is negatively associated with immune infiltration and negatively related to CD8+ T cells, CD4+ T cells, macrophages, neutrophil cells, and dendritic cells. The *FGL1* mutation analysis indicated that the main mutation

of *FGL1* was deep deletion, and the altered group had poor prognosis. The *FGL1* survival analysis indicated that *FGL1* was a risk factor in LUAD and predicted the poor prognosis of patients with LUAD. To further understand *FGL1*, we explored the gene-gene and protein-protein interactive networks and found that *FGL1* might interact with *LAG3*, *FGG*, *FGB*, *FGA*, and *ANGPT1*. *FGL1* might also interact with *LAG3* by physical interaction, but the functions between the two were unclear.

Third, our results showed that downregulation of *FGL1* affects *MYC*-target genes. SiRNA and shRNA were used to construct an *FGL1* knockdown with transient transfection and stable transfection in cell lines of PC9 and HCC827 lung cancer cells. After co-culture of PC9 cells and Jurkat T cells, the RNA-seq analysis showed that in PC9 cells, the knockdown of *FGL1* upregulated 953 genes and downregulated 408 genes but had little effect on Jurkat T cells. The differential genes were mainly enriched in *MYC*-target genes, which were tightly associated with cell proliferation, cell cycle, and apoptosis, similar result of RNA-seq was confirmed in HCC827 cells. Therefore, the downregulation of *FGL1* inhibits LUAD cell proliferation via regulating *MYC*-target genes.

After co-culture of PC9 cells and Jurkat T cells, the results of the cell cycle analysis, colony formation assay, and real-time cell analyzer all showed that cell proliferation of PC9 cells in the Co-Culture_LUAD-KD group was significantly decreased compared with that in the Co-Culture_LUAD-NC group, but that the proliferation of Jurkat T cells was hardly affected. As previous study has reported, the activation of the T cell receptor (TCR) on the membrane of Jurkat T cells is associated with entry into the cell cycle (37). Therefore, the fact that there was no any influence on Jurkat T cells after co-culture could be attributed to the inactivation of TCR on Jurkat T cells. To eliminate the effects of co-culture, we analyzed the PC9 cells of LUAD-NC and LUAD-KD. Similar results were found in the LUAD-KD group, which indicated that the downregulation of *FGL1* inhibits the proliferation of LUAD cells.

In conclusion, we confirmed that *FGL1* is mainly accumulated in the cytoplasm of LUAD cells. While *FGL1* may act as an immune checkpoint in other diseases, it serves in LUAD proliferation by regulating *MYC*-target genes which provided the rationale to explore the upstream and downstream pathways related to *FGL1*, it also provided the therapeutic target for immunotherapy of LUAD and may help to improve the prognosis of patients.

Acknowledgments

Footnote

Reporting Checklist: The authors have completed the MDAR reporting checklist. Available at https://tlcr.amegroups.com/article/view/10.21037/tlcr-22-151/rc

Data Sharing Statement: Available at https://tlcr.amegroups.com/article/view/10.21037/tlcr-22-151/dss

Conflicts of Interest: All authors have completed the ICMJE uniform disclosure form (available at https://tlcr.amegroups.com/article/view/10.21037/tlcr-22-151/coif). The authors have no conflicts of interest to declare.

Ethical Statement: The authors are accountable for all aspects of the work in ensuring that questions related to the accuracy or integrity of any part of the work are appropriately investigated and resolved. The study was conducted in accordance with the Declaration of Helsinki (as revised in 2013). The study was approved by the Ethics Committee of the Air Force Medical University (No. 202003-018). Written informed consent, which included agreement to the use personal clinical data and the collection of tissue and plasma samples, was signed by all patients before any study-related procedures began.

References

1. Lin A, Wei T, Meng H, et al. Role of the dynamic tumor microenvironment in controversies regarding immune checkpoint inhibitors for the treatment of non-small cell lung cancer (NSCLC) with EGFR mutations. Mol Cancer 2019;18:139.

2. Siegel RL, Miller KD, Fuchs HE, et al. Cancer statistics, 2022. CA Cancer J Clin 2022;72:7-33.

3. Pasello G, Pavan A, Attili I, et al. Real world data in the era of Immune Checkpoint Inhibitors (ICIs): Increasing evidence and future applications in lung cancer. Cancer Treat Rev 2020;87:102031.

4. Zhang Y, Qiao HX, Zhou YT, et al. Fibrinogen like protein 1 promotes the invasion and metastasis of gastric cancer and is associated with poor prognosis. Mol Med Rep 2018;18:1465-72.

5. Visan I. New ligand for LAG-3. Nat Immunol 2019;20:111.

6. Xu F, Liu J, Liu D, et al. LSECtin expressed on melanoma cells promotes tumor progression by inhibiting antitumor T-cell responses. Cancer Res 2014;74:3418-28.

7. Kouo T, Huang L, Pucsek AB, et al. Galectin-3 Shapes Antitumor Immune Responses by Suppressing CD8+ T Cells via LAG-3 and Inhibiting Expansion of Plasmacytoid Dendritic Cells. Cancer Immunol Res 2015;3:412-23.

8. Graydon CG, Mohideen S, Fowke KR. LAG3's Enigmatic Mechanism of Action. Front Immunol 2021;11:615317.

9. Du H, Yi Z, Wang L, et al. The co-expression characteristics of LAG3 and PD-1 on the T cells of patients with breast cancer reveal a new therapeutic strategy. Int Immunopharmacol 2020;78:106113.

10. Wang J, Sanmamed MF, Datar I, et al. Fibrinogen-like Protein 1 Is a Major Immune Inhibitory Ligand of LAG-3. Cell 2019;176:334-347.e12.

11. Guo M, Yuan F, Qi F, et al. Expression and clinical significance of LAG-3, FGL1, PD-L1 and CD8+T cells in hepatocellular carcinoma using multiplex quantitative analysis. J Transl Med 2020;18:306.

12. Sun C, Gao W, Liu J, et al. FGL1 regulates acquired resistance to Gefitinib by inhibiting apoptosis in non-small cell lung cancer. Respir Res 2020;21:210.

13. Zhou J, Yu X, Hou L, et al. Epidermal growth factor receptor tyrosine kinase inhibitor remodels tumor microenvironment by upregulating LAG-3 in advanced non-small-cell lung cancer. Lung Cancer 2021;153:143-9.

14. Bie F, Wang G, Qu X, et al. Loss of FGL1 induces epithelial mesenchymal transition and angiogenesis in LKB1 mutant lung adenocarcinoma. Int J Oncol 2019;55:697-707.

15. Liu XS, Gao Y, Liu C, et al. Comprehensive Analysis of Prognostic and Immune Infiltrates for E2F Transcription

Factors in Human Pancreatic Adenocarcinoma. Front Oncol 2021;10:606735.

16. Tang XY, Shi AP, Xiong YL, et al. Clinical Research on the Mechanisms Underlying Immune Checkpoints and Tumor Metastasis. Front Oncol 2021;11:693321.

17. Rhodes DR, Kalyana-Sundaram S, Mahavisno V, et al. Oncomine 3.0: genes, pathways, and networks in a collection of 18,000 cancer gene expression profiles. Neoplasia 2007;9:166-80.

18. Chen F, Chandrashekar DS, Scheurer ME, et al. Global molecular alterations involving recurrence or progression of pediatric brain tumors. Neoplasia 2022;24:22-33.

19. Chen F, Chandrashekar DS, Varambally S, et al. Pan-cancer molecular subtypes revealed by mass-spectrometry-based proteomic characterization of more than 500 human cancers. Nat Commun 2019;10:5679.

20. Chandrashekar DS, Bashel B, Balasubramanya SAH, et al. UALCAN: A Portal for Facilitating Tumor Subgroup Gene Expression and Survival Analyses. Neoplasia 2017;19:649-58.

21. Cerami E, Gao J, Dogrusoz U, et al. The cBio cancer genomics portal: an open platform for exploring multidimensional cancer genomics data. Cancer Discov 2012;2:401-4.

22. Gao J, Aksoy BA, Dogrusoz U, et al. Integrative analysis of complex cancer genomics and clinical profiles using the cBioPortal. Sci Signal 2013;6:pl1.

23. Warde-Farley D, Donaldson SL, Comes O, et al. The GeneMANIA prediction server: biological network integration for gene prioritization and predicting gene function. Nucleic Acids Res 2010;38:W214-20.

24. Szklarczyk D, Gable AL, Nastou KC, et al. The STRING database in 2021: customizable protein-protein networks, and functional characterization of user-uploaded gene/measurement sets. Nucleic Acids Res 2021;49:D605-12.

25. Li T, Fu J, Zeng Z, et al. TIMER2.0 for analysis of tumor-infiltrating immune cells. Nucleic Acids Res 2020;48:W509-14.

26. Li T, Fan J, Wang B, et al. TIMER: A Web Server for Comprehensive Analysis of Tumor-Infiltrating Immune Cells. Cancer Res 2017;77:e108-10.

27. Barrett T, Wilhite SE, Ledoux P, et al. NCBI GEO: archive for functional genomics data sets--update. Nucleic Acids Res 2013;41:D991-5.

28. Mizuno H, Kitada K, Nakai K, et al. PrognoScan: a new database for meta-analysis of the prognostic value of genes.

BMC Med Genomics 2009;2:18.

29. Subramanian A, Tamayo P, Mootha VK, et al. Gene set enrichment analysis: a knowledge-based approach for interpreting genome-wide expression profiles. Proc Natl Acad Sci U S A 2005;102:15545-50.

30. Mootha VK, Lindgren CM, Eriksson KF, et al. PGC-1alpha-responsive genes involved in oxidative phosphorylation are coordinately downregulated in human diabetes. Nat Genet 2003;34:267-73.

31. Kim S, Jang JY, Koh J, et al. Programmed cell death ligand-1-mediated enhancement of hexokinase 2 expression is inversely related to T-cell effector gene expression in non-small-cell lung cancer. J Exp Clin Cancer Res 2019;38:462.

32. Morton LM, Purdue MP, Zheng T, et al. Risk of non-Hodgkin lymphoma associated with germline variation in genes that regulate the cell cycle, apoptosis, and lymphocyte development. Cancer Epidemiol Biomarkers Prev 2009;18:1259-70.

33. Qian W, Zhao M, Wang R, et al. Fibrinogen-like protein 1 (FGL1): the next immune checkpoint target. J Hematol Oncol 2021;14:147.

34. Sun C, Mezzadra R, Schumacher TN. Regulation and Function of the PD-L1 Checkpoint. Immunity 2018;48:434-52.

35. Nayeb-Hashemi H, Desai A, Demchev V, et al. Targeted disruption of fibrinogen like protein-1 accelerates hepatocellular carcinoma development. Biochem Biophys Res Commun 2015;465:167-73.

36. Lehtiö J, Arslan T, Siavelis I, et al. Proteogenomics of non-small cell lung cancer reveals molecular subtypes associated with specific therapeutic targets and immune evasion mechanisms. Nat Cancer 2021;2:1224-42.

37. Abraham RT, Weiss A. Jurkat T cells and development of the T-cell receptor signalling paradigm. Nat Rev Immunol 2004;4:301-8.

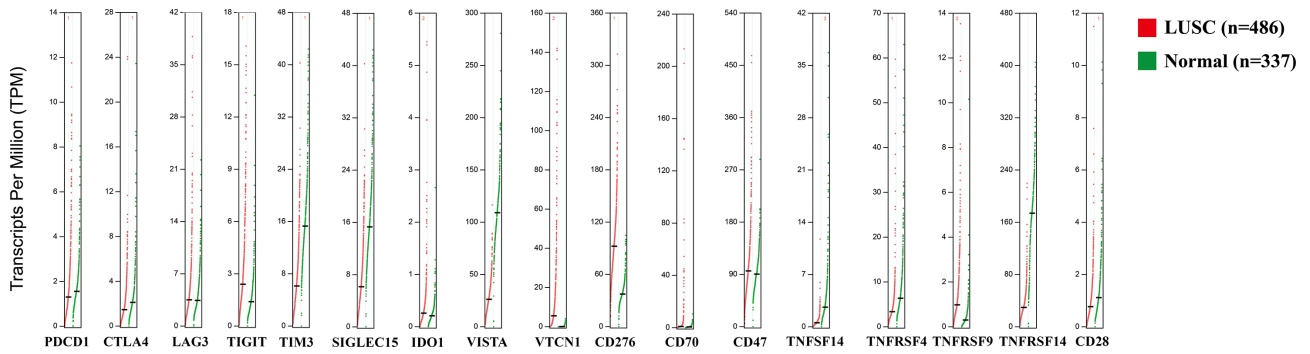(English Language Editor: C. Gourlay)

Figure S1 The mRNA expression of 17 receptors were explored in LUSC. LUSC, lung squamous carcinoma.
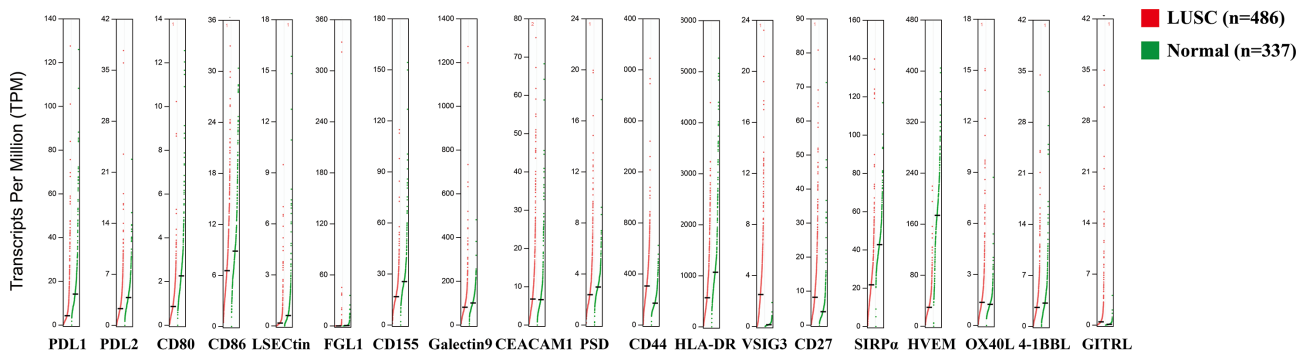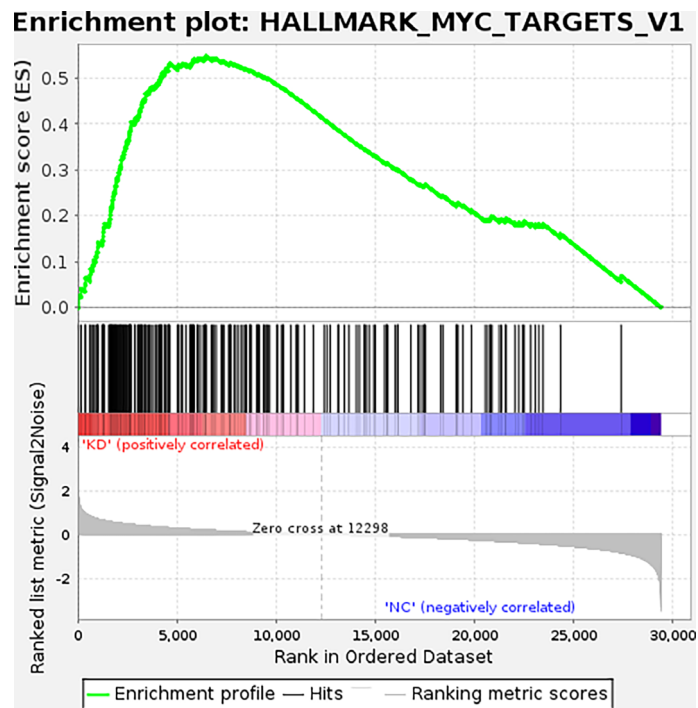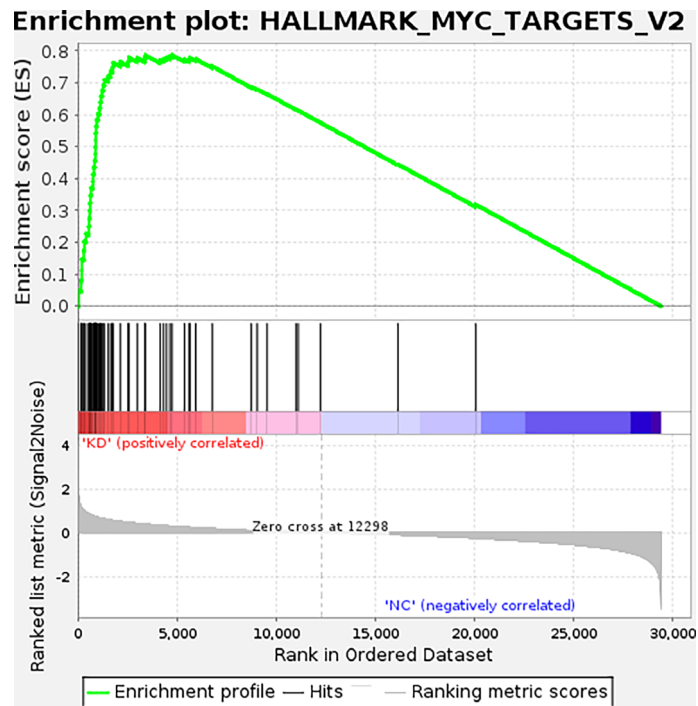

Figure S2 The corresponding 19 ligands were explored in LUSC. LUSC, lung squamous carcinoma.

Figure S3 The enrichment plot of *MYC_target_v1* in HCC827 cells after *FGL1* knockdown.

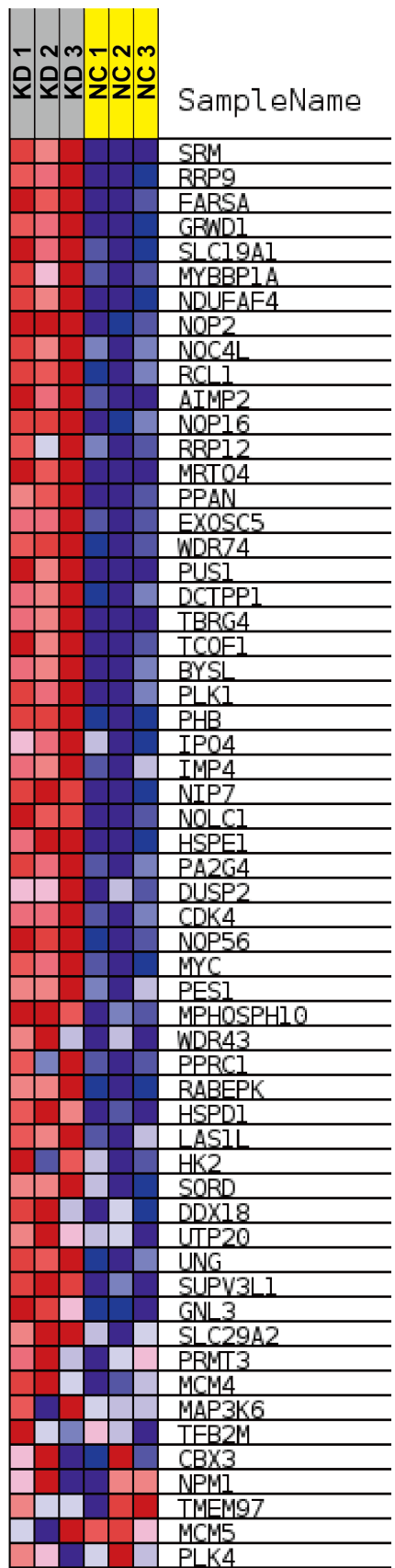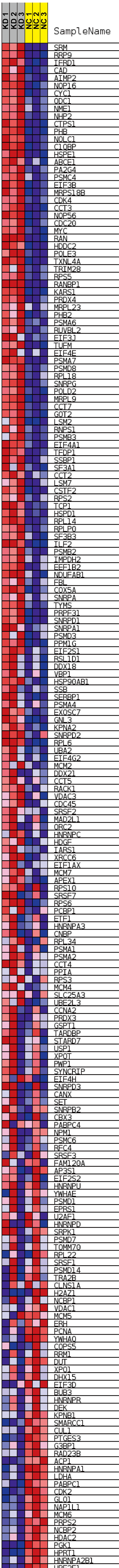**Figure S4** *MYC_target_v2* in HCC827 cells after *FGL1* knockdown.

Figure S5 (left heat map) — SampleName:

SRM, RRP9, IFRD1, CAD, AIMP2, NOP16, CYC1, ODC1, NME1, NHP2, CTPS1, PHB, NOLC1, C1QBP, HSPE1, ABCE1, PA2G4, PSMC4, EIF3B, MRPS18B, CDK4, CCT3, NOP56, CDC20, MYC, RAN, HDDC2, POLE3, TXNL4A, TRIM28, RPS5, RANBP1, KARS1, PRDX4, MRPL23, PHB2, PSMA6, RUVBL2, EIF3J, TUFM, EIF4E, PSMA7, PSMD8, RPL18, SNRPG, POLD2, MRPL9, CCT7, GOT2, LSM2, RNPS1, PSMB3, EIF4A1, TFDP1, SSBP1, SF3A1, CCT2, LSM7, CSTF2, RPS2, TCP1, HSPD1, RPL14, RPLP0, SF3B3, ILF2, PSMB2, IMPDH2, EEF1B2, NDUFAB1, FBL, COX5A, SNRPA, TYMS, PRPF31, SNRPD1, SNRPA1, PSMD3, PPM1G, EIF2S1, RSL1D1, DDX18, VBP1, HSP90AB1, SSB, SERBP1, PSMA4, EXOSC7, GNL3, KPNA2, SNRPD2, RPL6, UBA2, EIF4G2, MCM2, DDX21, CCT5, RACK1, VDAC3, CDC45, SRSF2, MAD2L1, ORC2, HNRNPC, HDGF, IARS1, XRCC6, EIF1AX, MCM7, APEX1, RPS10, SRSF7, RPS6, PCBP1, ETF1, HNRNPA3, CNBP, RPL34, PSMA1, PSMA2, CCT4, PPIA, RPS3, MCM4, SLC25A3, UBE2L3, CCNA2, PRDX3, GSPT1, TARDBP, STARD7, USP1, XPOT, PWP1, SYNCRIP, EIF4H, SNRPD3, CANX, SET, SNRPB2, CBX3, PABPC4, NPM1, PSMC6, RFC4, SRSF3, FAM120A, AP3S1, EIF2S2, HNRNPU, YWHAE, PSMD1, EPRS1, U2AF1, HNRNPD, SRPK1, PSMD7, TOMM70, RPL22, SRSF1, PSMD14, TRA2B, CLNS1A, H2AZ1, NCBP1, VDAC1, MCM5, ERH, PCNA, YWHAQ, COPS5, RRM1, DUT, XPO1, DHX15, EIF3D, BUB3, HNRNPR, DEK, KPNB1, SMARCC1, CDC1, PTGES3, G3BP1, RAD23B, ACP1, HNRNPA1, LDHA, PABPC1, CDK2, GLO1, NAP1L1, MCM6, RRP52, NCBP2, HDAC2, PGK1, HPRT1, HNRNPA2B1, UBE2E1

Figure S6 (right heat map) — SampleName:

SRM, RRP9, FARSA, GRWD1, SLC19A1, MYBBP1A, NDUFAF4, NOP2, NOC4L, RCL1, AIMP2, NOP16, RRP12, MRTO4, PPAN, EXOSC5, WDR74, PUS1, DCTPP1, TBRG4, TCOF1, BYSL, PLK1, PHB, IPO4, IMP4, NIP7, NOLC1, HSPE1, PA2G4, DUSP2, CDK4, NOP56, MYC, PES1, MPHOSPH10, WDR43, PPRC1, RABEPK, HSPD1, LAS1L, HK2, SORD, DDX18, UTP20, UNG, SUPV3L1, GNL3, SLC29A2, PRMT3, MCM4, MAP3K6, TFB2M, CBX3, NPM1, TMEM97, MCM5, PLK4

Figure S6 Heat map of *MYC_target_v2* in HCC827 cells after *FGL1* knockdown.

Figure S5 Heat map of *MYC_target_v1* gene in HCC827 cells after *FGL1* knockdown.